Scripta Materialia 182 (2020) 94–98

Contents lists available at ScienceDirect

Scripta Materialia

journal homepage: www.elsevier.com/locate/scriptamat

Electrode-**dependent** Joule heating in soda lime silicate glass during flash processes

Mattia Biesuz*, Mattia Cipriani, Vincenzo M. Sglavo, Gian D. Sorarù

University of Trento, Department of Industrial Engineering, Via Sommarive 9, 38123 Trento, Italy

ARTICLE INFO

Article history:
Received 13 February 2020
Revised 27 February 2020
Accepted 2 March 2020
Available online 13 March 2020

Keywords:
Joule heating
Flash sintering
Soda lime glass
Electric field
Electric field-induced softening

ABSTRACT

Electric current-assisted technologies stand as a promising route to reduce the carbon footprint of the 21st century industry. Nevertheless, recent activities on flash sintering have shown that electrically-induced DC Joule heating in silicate glasses is highly inhomogeneous under the effect of a direct electric field, thus limiting further developments and industrial applications. In this work, we have shown that the Joule heating in soda lime silicate glass can be tailored and controlled by changing the material used as electrode. The highly inhomogeneous temperature profile developed using platinum electrodes turns into a well-homogenous distribution by employing molten $NaNO_3$ electrodes.

The identification of the potential electric energy conversion into heat dates back to 1841 when J.P. Joule [1] observed that "*when a current of voltaic electricity is propagated […], the heat evolved […] is proportional to the resistance of the conductor multiplied by the square of the electric* (current) *intensity*" [1]. The phenomenon, named "Joule heating", is based on the momentum transfer from the charge particles (accelerated under the effect of the external electric field) to the lattice, which is therefore heated [2]. Since then, the Joule heating has been recognized as a powerful tool to enhance materials processing as it allows unconventionally rapid and localized heating. Electric current-assisted processes (ECAPs) are nowadays widely employed in the field of metals manufacturing. As an example, resistance welding techniques like, for example, spot [3], seam [4], projection welding [5] played a fundamental role for the development of the modern and highly automated automotive manufacturing [6]. Other examples of ECAPs based on the Joule heating are induction heating systems [7] and field-assisted sintering [8–10].

The key advantage of ECAPs lays on the fact that the heat is internally generated, thus allowing to reduce the total energy consumption of the process. Moreover, the reduced processing time allows to confine the heat and preserve microstructural features that might degrade at high temperature [11]. For these reasons ECAPs represent a promising tool to reduce the carbon footprint of the 21st century manufacture and provide a tool to manipulate out-of-equilibrium/metastable systems [12–14].

On the other hand, Joule heating-based ECAPs are only of marginal interest for ceramic and glass manufacturing as such materials are generally (although, not always) insulators at room temperature. Nevertheless, the recent research activities on flash sintering (FS) [9,15–17], reactive flash sintering [18–21] and flash joining [22–25] of ceramics have disclosed new opportunities. Herein, the material is subjected to an external electric field and heated within a conventional furnace until it is hot enough to sustain a thermal runaway of the Joule heating [26,27], which can be however coupled with other athermal effects [28–32]. In parallel, McLaren, Jane and co-workers carried out research activities on the so-called electric field-induced softening (EFIS) where bulk alkali silicate glasses are subjected to a flash process which triggers viscous flow [33,34]. Nonetheless, the Joule heating in such materials resulted highly inhomogeneous [35,36], the positive electrode being always overheated. Thermal gradients upon FS have been also reported in ionic conductive ceramics, such as yttria-stabilized zirconia [37–39].

Recent research activities on FS have shown that the thermal runaway of Joule heating in ionic conductors can be altered by changing the electrode configuration [38,40,41]. In the present letter we aimed to understand whether the electrode material choice changes the Joule heating behavior in the world-most-diffuse vitreous material (soda lime silicate glass) and whether it could be made homogeneous.

A commercial soda lime silicate float glass was used in this work with composition (wt%): 71.4 SiO_2; 1.0 Al_2O_3; 13.9 Na_2O;

* Corresponding author.
E-mail address: mattia.biesuz@unitn.it (M. Biesuz).

https://doi.org/10.1016/j.scriptamat.2020.03.005
1359-6462/

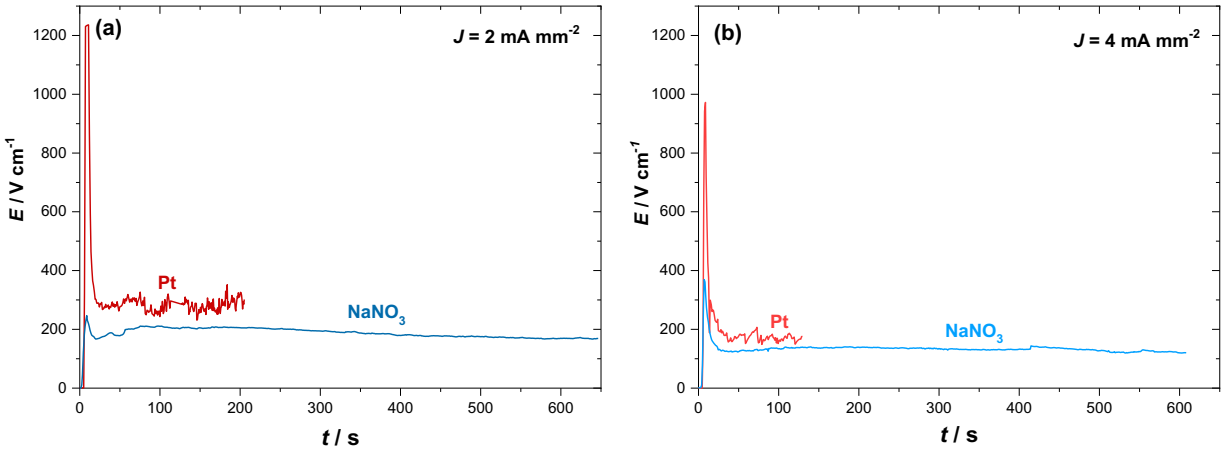

Fig. 1. Electric field (averaged over the gage length) applied on soda lime silicate glass samples using Pt and molten $NaNO_3$ electrodes at different current densities: (a) 2 mA mm^{-2} and (b) 4 mA mm^{-2}.

0.3 K_2O; 4.1 MgO; 9.1 CaO; 0.2 others. The glass transition temperature (T_g = 568 °C) and the dilatometric softening point of the glass (T_s = 611 °C) were evaluated using a Linseis L75 silica dilatometer at 5 °C min^{-1} and 12 kPa.

Bar-like specimens 20.0 ± 1.5 mm long with a square cross-section of 16.0 ± 2.0 mm^2 were cut from the glass sheets. The samples were introduced within a fused silica tube and placed in contact with the electrodes. Two different electrode configurations were used: (i) the square faces of the glass sample were painted with Pt paste (C60903P5 Gwent) and connected to two 90Pt-10Rh disks (diameter = 9 mm); (ii) the same configuration was reproduced for the cathode (-) whereas the anode (+) was soaked in ≈ 3 mm of molten $NaNO_3$ (Figs. 2,3). The two electrode configurations will be simply named as "Pt electrode" and "$NaNO_3$ electrode" in the followings.

The glass was then heated at 400 ± 15 °C by a heat gun in ambient air. The temperature was checked with a K-thermocouple placed close to the sample before all experiments. An increasing DC electric field was applied using a Glassman EW series 5 kV–120 mA power supply until the flowing current reached the limit of the power source (set at 0.3–4 mA mm^{-2}). Then, the heat gun was turned off: in this way, the sample overheating with respect to room temperature could be attributed to the internal heat generation by the Joule effect, only.

The electric data (current and voltage) were recorded using a Keithley-2100 digital multimeter (acquisition frequency = 1 Hz). The experiments were filmed with a digital camera Canon EOS-750D and with a thermocamera FLIRT-T62101. The emissivity was set 0.97 in accordance with the manufacturer suggestion for silicate glassy materials. The agreement between the temperature measured by the thermocamera and the real one was additionally checked with a thermocouple before starting the experiments.

Fig. 1 compares the average electric field measured along the glass samples for current of 2 and 4 mA mm^{-2}. One can observe the presence of an E field spike at the beginning of the experiments which allows to initiate the current flow. After that, the current starts to flow, the sample is electrically heated and its resistivity decreases, thus causing a reduction the applied field (non-metallic compounds exhibit a negative temperature coefficient for resistivity). Interestingly, the electric behavior appears rather different for the two types of electrode. In particular, we can observe that:

i. The field needed to initiate the current flow (i.e., the dielectric strength) is extremely different, it being more than doubled in case of Pt electrodes compared with $NaNO_3$.
ii. The field drop after the current starts to flow is much more pronounced when using Pt electrodes.
iii. In the "steady stage" after the current spike, the field is slightly higher when using Pt anode.
iv. The electric field is extremely unstable and noisy when Pt electrodes are employed. Conversely, the E vs. t plot is stable and smooth using molten $NaNO_3$ anode.

These results point out that the electric behavior of soda lime silicate glass is complex and it is not a simple function of T and composition, but it also depends on the electrode material choice.

Indeed, the differences in terms of electric conductivity, dielectric strength, field stability impact also on the Joule heating of the glass (Figs. 2 and 3). The samples with Pt electrodes (Fig. 2) showed a very bright glowing from the anodic region (+) which is coupled with the development of a moving bright-hot spot within the glass (close to the anode). The spot is generated since the very beginning of the experiments ("Supplementary material", Video S1-8), just after that the current starts to flow. It is characterized by a significant overheating with respect to the other regions of the sample (hundreds of degrees) as shown in Fig. 4. The size and temperature of the bright hot spot indeed depend on the applied current, but it is clearly visible also in case at very small currents (i.e., 0.3 mA mm^{-2}). The bright glowing from the anode can be attributed to the combined effect of black body radiation and emission from luminescent centres located on the alkalis in the glass, namely Na at 589 and K at 769 nm (inset in Fig. 4a). Similar effects have already been reported by Pinter et al. [35]. and McLaren et al. [36]. in alkali-containing silicate glasses heated under DC using Pt wires and graphite disks as electrodes, respectively. It is however worth mentioning that they used significantly larger current limits, 13 mA mm^{-2} [35] and 20 mA mm^{-2} [36]. Therefore, the present work shows that the Joule heating in soda lime silicate glass is extremely unstable even in case of very moderate current applications (i.e., 0.3 mA mm^{-2}), which are about two orders of magnitude lower than that reported in the previous works.

The hot spot origin has been already unraveled in [35,36,42], where it was correlated with the formation of an alkali depletion layer close to the anode (+) due to alkalis migration toward the cathode (−), as proved by the EDS analysis in Fig. 4c. This causes a local increase of the glass resistivity at the anode (being soda lime silicate glass an alkali ions conductor [43,44]) and consequently an E intensification (≈ 10^6–10^7 V cm^{-1} [36]) producing dielectric breakdown [45] of the silica-based network. The non-uniform glass composition/electric properties under DC field causes the inhomogeneous Joule heating (Fig. 2). One can note that the hot spot

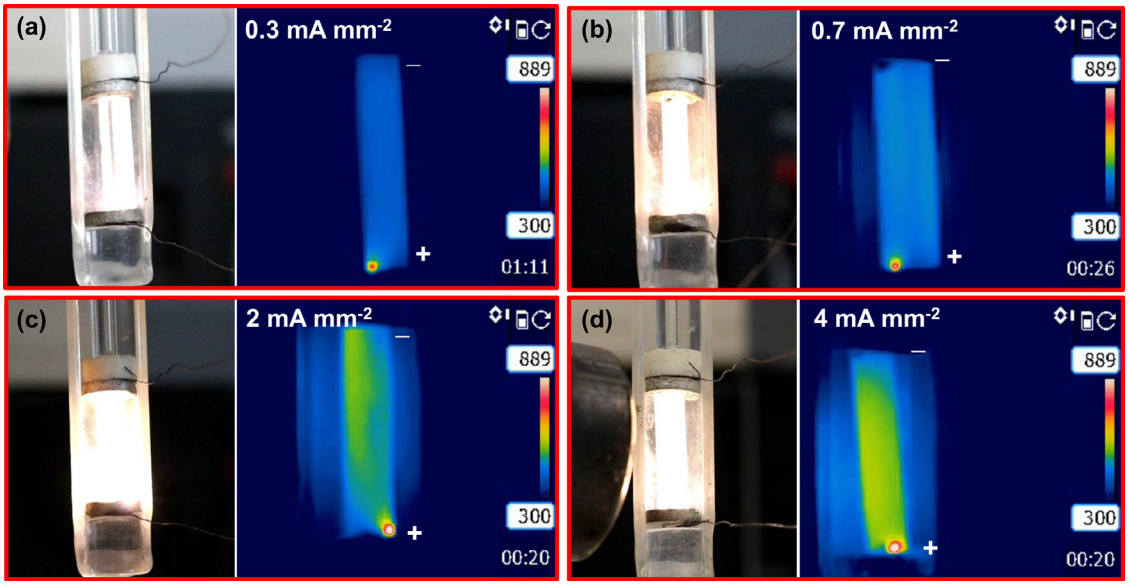

Fig. 2. Digital camera and thermocamera video stills of soda lime glass subjected to (a) 0.3 mA mm^{-2}, (b) 0.7 mA mm^{-2}, (c) 2 mA mm^{-2} and (d) 4 mA mm^{-2} using solid Pt electrodes.

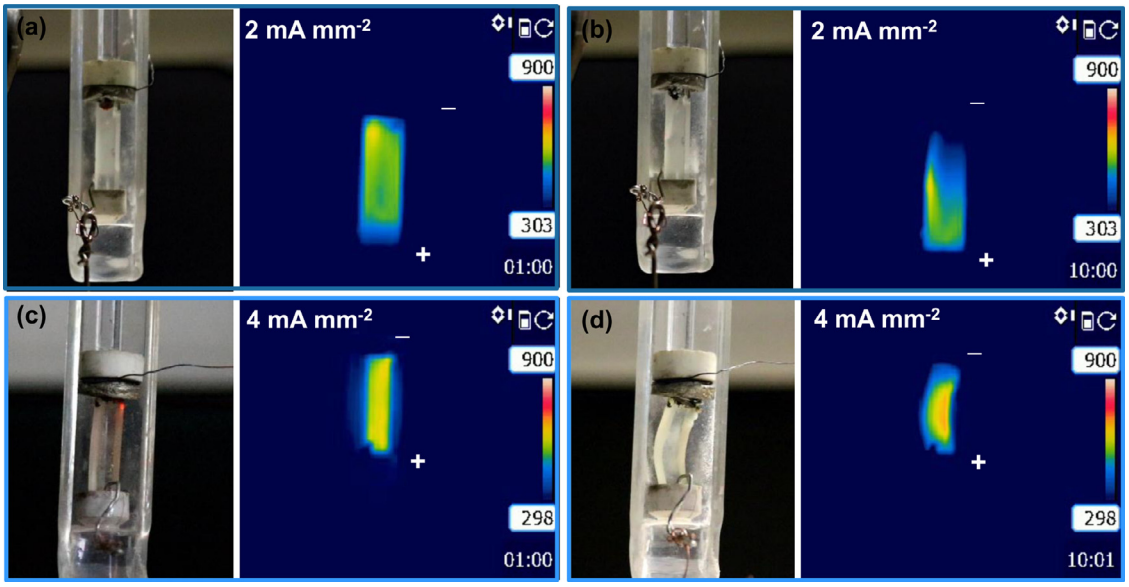

Fig. 3. Digital camera and thermocamera video stills of soda lime silicate glass subjected to (a, b) 2 mA mm^{-2} and (c, d) 4 mA mm^{-2} using molten $NaNO_3$ electrode at the anode side (+). (a, c) and (b, d) report the pictures of the samples 1 min and 10 min after the beginning of the experiment, respectively.

moves inside the specimen because the current concentrates in the region where the depletion layer is thinner at a given time [36]. This leads to a continuous movement of the current path which in turns originates the abrupt fluctuations in the *E* values reported in Fig. 1 (and Fig. 1S in "Supplementary material").

The most important finding of this work is represented by the results reported in Figs. 3 and 4b, where it is shown that the floating hot spot in the anodic region completely disappears when the anode is constituted by molten $NaNO_3$ (see also "Supplementary material", Video S9-12). The hot spot does not appear even in case of prolonged treatments (i.e., 10 min) at relatively high currents (i.e., 4 mA mm^{-2}). This is an obvious consequence of the fact that the alkali ions moving toward the cathode (-) are replaced in the anodic region by Na^+ ions from the salt bath (similarly to field-assisted ion exchange processes [46,47]). Under such conditions, the highly resistive alkali depletion layer at the anode (+) is not formed. Fig. 4d clearly shows that the anodic region maintains substantially the same composition of the original glass in case of molten $NaNO_3$ electrode. Conversely, the Na signal at the anode is definitively weakened in case of Pt electrode. From an electrochemical point of view we can observe that, when using Pt anodes, the Na^+ migration should be counterbalance by molecular oxygen evolution:

$$O^{2-} \rightarrow 2e^- + \frac{1}{2}O_{2(g)} \quad (1)$$

and by the formation of free electrons that are promptly collected at the metal electrode (+). The generation of electronic disorder in the alkali depletion layer might also contribute to the activation of electronic conductivity in the glass. On the other hand, in case of $NaNO_3$ anodes, the charge carriers are ionic both in the glass and in the salt electrode. Thus, there is a simple substitution of Na^+ from the salt into the glass. In this case, the conversion of ionic to electronic current moves at the interface between the Pt wire and

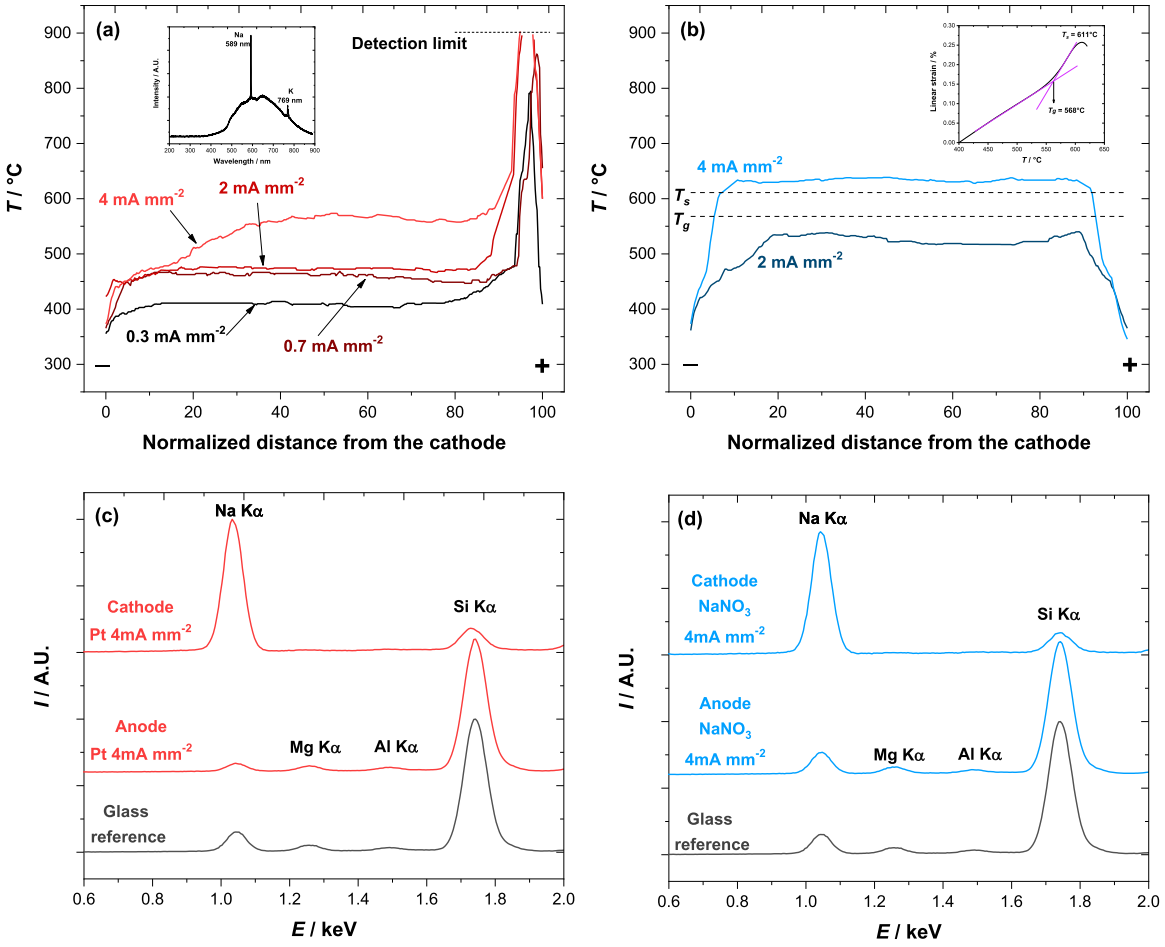

Fig. 4. Temperature profiles obtained using (a) Pt and (b) molten $NaNO_3$ electrodes (data extracted from Fig. 2a–d and Fig. 3a and c). The inset in (a) reports the photoemission from the specimen recorded while using Pt electrodes ($J = 2$ mA mm^{-2}), whereas the inset in (b) shows the dilatometric plot of the glass evidencing the T_g and T_s. The EDS spectra obtained on the glass after treatments using Pt and molten $NaNO_3$ electrodes are reported in (c) and (d), respectively.

the molten $NaNO_3$ where electrons are released by the oxidation of the nitrate forming nitrogen oxides and molecular oxygen. It is worth mentioning that in both cases a clear accumulation of Na at the cathode takes place; here the conversion from ionic (in the glass) to electronic (in Pt) current likely involves the reduction of sodium ions [44]. We did not see any reason against the possibility of using molten $NaNO_3$ cathodes in the next future to eliminate such local alkali species accumulation.

For these reasons the use of molten $NaNO_3$ anode allows a rather homogeneous heating of the glass specimen. Moreover, the absence of the hot spot leads to the disappearance of the strong E fluctuations observed in Fig. 1. We can therefore deduce that the DC Joule heating intensity and distribution in alkali-containing glasses strongly depend on the electrode configuration and it can be made homogenous simply by employing electrodes acting as alkali suppliers.

The presence/absence of the alkali depletion layer also explains the dielectric strength differences (i.e. the E spike in Fig. 1) when using Pt or molten $NaNO_3$ anodes. In fact, in case of Pt electrode the current flow can be initiated only by breaking the highly resistive SiO_2 layer at the anode, thus increasing the average electric field required for breakdown. Once the SiO_2 layer breaks, sample resistance strongly decreases, leading to the abrupt drop of E observed in Fig. 1 for the case of Pt electrode (the E decrease being much less pronounced when using molten $NaNO_3$ anode). Therefore, not only the Joule heating but also the dielectric strength of the glass appears dependent on the electrode material choice.

We can also point out that the yellowish-orange luminescence related to the emission lines of Na and K observed with Pt electrodes completely disappears using molten $NaNO_3$. The luminescent lines are therefore excited within the hot spot by the local high temperature (and, very likely, by the formation of electronic disorder under high field strength at the anode). Therefore, the presence of luminescence upon EFIS can be merely attributed to extremely localized effects related to the formation of chemical inhomogeneity under DC.

Finally, it is worth spotting that the sample treated with $NaNO_3$ anode at 2 mA mm^{-2} is not deformed during the process; conversely, the specimen treated at 4 mA mm^{-2} is highly bended after 10 min current flow (Fig. 3). Such result is in perfect agreement with the thermocamera measurement, which suggests that the former remained ≈40 °C below the T_g and the latter was ≈20 °C above the T_s of the glass. The results point out that EFIS using molten $NaNO_3$ anode is primarily a thermal phenomenon with only limited (or none) athermal effects of the field/current on the glass rheology. Definitive conclusion for the case of Pt electrodes cannot be drawn because of the unstable and inhomogeneous heating.

In summary, the simple picture stating that the Joule heating only depends on the material properties and temperature, fails when it is applied to soda lime silicate glasses under DC experiments. Here, the Joule heating and the electric properties are highly influenced by the choice of the electrode material. Electrodes able to supply alkali ions to the glass (like molten $NaNO_3$)

lead to homogeneous Joule heating under DC, whereas inert electrodes (like Pt) cause the development of strong thermal gradients associated to localized overheating of the anodic region.

Declaration of Competing Interest

The authors declare that they have no known competing financial interests or personal relationships that could have appeared to influence the work reported in this paper.

Acknowledgements

The authors warmly acknowledge Prof. Stefano Gialanella, Prof. Alberto Quaranta, Dr. Mara Leonardi and Mr. Lorenzo Pinter for the collaboration. V.M. Sglavo, M. Biesuz and G.D Sorarù kindly acknowledge the support from the Italian Ministry of University and Research (MIUR) within the programs PRIN2017 - 2017FCFYHK "DIRECTBIOPOWER", PRIN2017 - 2017PMR932 "Nanostructured Porous Ceramics for Environmental and Energy Applications" and Departments of Excellence 2018–2022 (DII-UNITN).

Supplementary materials

Supplementary material associated with this article can be found, in the online version, at doi:10.1016/j.scriptamat.2020.03.005.

References

[1] J.P. Joule, Edinburgh London, Dublin Philos, Mag. J. Sci. 19 (1841) 260–277.
[2] J.P. Hartnett, Advances in Heat Transfer, 37, Elsevier Ltd, UK, 2003.
[3] T.W. Neville, ASM - Handbook-, 6, ASM International, 1993.
[4] M.J. Karagoulis, ASM - Handbook-, 6, ASM International, 1993.
[5] J.E. Gould, ASM - Handbook-, 6, ASM International, 1993.
[6] N.T. Williams, J.D. Parker, Int. Mater. Rev. 49 (2004) 45–75.
[7] V. Rudnev, D. Loveless, R.L. Cook, Handbook of Induction Heating, 2nd ed., Taylor & Francis, n.d.
[8] R. Orrù, R. Licheri, A.M. Locci, A. Cincotti, G. Cao, Mater. Sci. Eng. R 63 (2009) 127–287.
[9] M. Yu, S. Grasso, R. Mckinnon, T. Saunders, M.J. Reece, Adv. Appl. Ceram. 116 (2017) 24–60.
[10] O. Guillon, J. Gonzalez-Julian, B. Dargatz, T. Kessel, G. Schierning, J. Räthel, M. Herrmann, Adv. Eng. Mater. 16 (2014) 830–849.
[11] M. Yu, T. Saunders, S. Grasso, A. Mahajan, H. Zhang, M.J. Reece, Scr. Mater. 146 (2018) 241–245.
[12] T.P. Mishra, R.R. Ingraci Neto, G. Speranza, A. Quaranta, V.M. Sglavo, R. Raj, O. Guillon, M. Bram, M. Biesuz, Scr. Mater. 179 (2020) 55–60.
[13] B.B. Kayaalp, K. Klauke, M. Biesuz, A. Iannaci, V.M. Sglavo, M. D'Arienzo, H. Noei, S. Lee, W. Jung, S. Mascotto, J. Phys. Chem. C 123 (2019) 16883–16892.
[14] W. Rheinheimer, X.L. Phuah, H. Wang, F. Lemke, M.J. Hoffmann, H. Wang, Acta Mater 165 (2019) 398–408.
[15] M. Cologna, B. Rashkova, R. Raj, J. Am. Ceram. Soc. 93 (2010) 3556–3559.
[16] M. Biesuz, V.M. Sglavo, J. Eur. Ceram. Soc. 39 (2019) 115–143.
[17] R. Muccillo, M. Kleitz, E.N.S.S. Muccillo, J. Eur. Ceram. Soc. 31 (2011) 1517–1521.
[18] Y. Wu, X. Su, G. An, W. Hong, Scr. Mater. 174 (2020) 49–52.
[19] D. Kok, D. Yadav, E. Sortino, S.J. McCormack, K.-P. Tseng, W.M. Kriven, R. Raj, M.L. Mecartney, J. Am. Ceram. Soc. 102 (2019) 644–653.
[20] B. Yoon, V. Avila, R. Raj, L.M. Jesus, Scr. Mater. 181 (2020) 48–52.
[21] E. Gil-González, A. Perejón, P.E. Sánchez-Jiménez, M.J. Sayagués, R. Raj, L.A. Pérez-Maqueda, Mater. Chem. A 6 (2018) 5356–5366.
[22] M. Biesuz, T.G. Saunders, S. Grasso, G. Speranza, G.D. Sorarù, R. Campostrini, V.M. Sglavo, M.J. Reece, J. Eur. Ceram. Soc. 39 (2019) 4664–4672.
[23] J. Xia, K. Ren, Y. Wang, Scr. Mater. 165 (2019) 34–38.
[24] P. Tatarko, S. Grasso, T.G. Saunders, V. Casalegno, M. Ferraris, M.J. Reece, J. Eur. Ceram. Soc. 37 (2017) 3841–3848.
[25] M. Biesuz, T.G. Saunders, K. Chen, M. Bortolotti, M. Salvo, S. Grasso, M.J. Reece, J. Eur. Ceram. Soc. (2019) IN PRESS, doi:10.1016/j.jeurceramsoc.2019.12.011.
[26] R.I. Todd, E. Zapata-Solvas, R.S. Bonilla, T. Sneddon, P.R. Wilshaw, J. Eur. Ceram. Soc. 35 (2015) 1865–1877.
[27] Y. Zhang, J. Il Jung, J. Luo, Acta Mater 94 (2015) 87–100.
[28] R. Chaim, Materials (Basel) 9 (2016) 19–21.
[29] R. Chaim, Scr. Mater. 158 (2019) 88–90.
[30] W. Ji, B. Parker, S. Falco, J.Y. Zhang, Z.Y. Fu, R.I. Todd, J. Eur. Ceram. Soc. 37 (2017) 2547–2551.
[31] M. Jongmanns, R. Raj, D.E. Wolf, New J. Phys. 20 (2018) 093013.
[32] R. Shi, Y. Pu, J. Ji, J. Li, X. Guo, W. Wang, M. Yang, Ceram. Int. (2020) IN PRESS, doi:10.1016/j.ceramint.2020.02.055.
[33] C. McLaren, W. Heffner, R. Tessarollo, R. Raj, H. Jain, Appl. Phys. Lett. 107 (2015) 1–6.
[34] C. McLaren, B. Roling, R. Raj, H. Jain, J. Non. Cryst. Solids 471 (2017) 384–395.
[35] L. Pinter, M. Biesuz, V.M. Sglavo, T. Saunders, J. Binner, M. Reece, S. Grasso, Scr. Mater. 151 (2018) 14–18.
[36] C.T. Mclaren, C. Kopatz, N.J. Smith, H. Jain, Sci. Rep. 9 (2019) 2805.
[37] G. Liu, D. Liu, J. Liu, Y. Gao, Y. Wang, J. Eur, Ceram. Soc. 7 (2018) 2893–2896.
[38] M. Biesuz, L. Pinter, T. Saunders, M. Reece, J. Binner, V.M. Sglavo, S. Grasso, Materials (Basel) 11 (2018) 1214.
[39] J.V. Campos, I.R. Lavagnini, R.V. de Sousa, J.A. Ferreira, E.M. de, J.A. Pallone, J. Eur. Ceram. Soc. 39 (2018) 531–538.
[40] L.B. Caliman, R. Bouchet, D. Gouvea, P. Soudant, M.C. Steil, J. Eur. Ceram. Soc. 36 (2016) 1253–1260.
[41] C.A. Grimley, A.L.G. Prette, E.C. Dickey, Acta Mater 174 (2019) 271–278.
[42] M.O. Prado, M. Biesuz, M. Frasnelli, F.E. Benedetto, V.M. Sglavo, J. Non. Cryst. Solids 476 (2017) 60–66.
[43] R.H. Doremus, Glass Science, II (1994).
[44] A.K. Varshneya, Fundamentals of Inorganic Glasses, Academic Press, Inc., 1994.
[45] J. Frenkel, Phys. Rev. 54 (1938) 647–648.
[46] N.A. Sanford, K.J. Malone, D.R. Larson, Opt. Lett. 15 (1990) 366–368.
[47] A. Talimian, G. Mariotto, V.M. Sglavo, Int. J. Appl. Glas. Sci. 8 (2017) 291–300.